



Swansea University
Prifysgol Abertawe



Cronfa - Swansea University Open Access Repository

This is an author produced version of a paper published in:
Sports Biomechanics

Cronfa URL for this paper:
<http://cronfa.swan.ac.uk/Record/cronfa48057>

Paper:

Ohshima, Y., Bezodis, N. & Nagahara, R. (2019). Calculation of the centre of pressure on the athletic starting block. *Sports Biomechanics*, 1-14.
<http://dx.doi.org/10.1080/14763141.2018.1561933>

This item is brought to you by Swansea University. Any person downloading material is agreeing to abide by the terms of the repository licence. Copies of full text items may be used or reproduced in any format or medium, without prior permission for personal research or study, educational or non-commercial purposes only. The copyright for any work remains with the original author unless otherwise specified. The full-text must not be sold in any format or medium without the formal permission of the copyright holder.

Permission for multiple reproductions should be obtained from the original author.

Authors are personally responsible for adhering to copyright and publisher restrictions when uploading content to the repository.

<http://www.swansea.ac.uk/library/researchsupport/ris-support/>

Calculation of the centre of pressure on the athletic starting block

Yuji Ohshima^a, Neil E. Bezodis^b, Ryu Nagahara^{c*}

- a) Institute for General Education, Ritsumeikan University, Kusatsu, Shiga, Japan
- b) Applied Sports, Technology, Exercise and Medicine Research Centre, Swansea University, Swansea, Wales, UK
ORCID: 0000-0003-2229-3310
- c) Sports Performance Research Center, National Institute of Fitness and Sports in Kanoya, Kanoya, Kagoshima, Japan
ORCID: 0000-0001-9101-9759

*Corresponding author:

Ryu Nagahara

Sports Performance Research Center, National Institute of Fitness and Sports in Kanoya

Address: 1 Shiromizu-cho, Kanoya, Kagoshima 891-2393, Japan

Tel: +81-994-46-5034

E-mail: nagahara@nifs-k.ac.jp

This study was conducted at the National Institute of Fitness and Sports in Kanoya.

Number of words (abstract): 200

Number of words (introduction to conclusion): 4599

Number of tables and figures: 5 figures and 2 tables

1 Calculation of the centre of pressure on the athletic starting block

2

3 **Abstract**

4 We aimed to evaluate the accuracy of a new method to calculate the centre of pressure (COP)
5 on a starting block above a force platform, and to examine how this method affected lower
6 extremity joint torques during the block clearance phase compared against a previously used
7 method which projects the COP from the metatarsophalangeal joint. To evaluate the accuracy
8 of the new method, one experimenter applied force at 18 known locations on a starting block
9 (under six block position and orientation conditions), during which ground reaction force was
10 recorded underneath using a force platform. Two sprinters then performed three block starts
11 each, and lower extremity joint torques were calculated during block clearance using the COP
12 obtained from the new method and from the projection of the metatarsophalangeal joint
13 location. The calculated COP using the new method had a mean bias of ≤ 0.002 m. There were
14 some large differences (effect sizes = 0.11–4.01) in the lower extremity joint torques between
15 the two methods which could have important implications for understanding block clearance
16 phase kinetics. The new method for obtaining the COP on a starting block is highly accurate
17 and affects the calculation of joint torques during the block clearance phase.

18

19 **Key words:** ground reaction force, COP, sprint running, inverse dynamics, track and field

20

21 **Introduction**

22 Calculating net joint torque and power, as well as the contribution of muscular contractions to
23 whole body acceleration, are of great benefit for understanding the causes of movement. Such
24 calculations have been widely applied in the study of the start and early acceleration in
25 sprinting (Bezodis, Salo, & Trewartha, 2014; Brazil et al., 2017; 2018; Charalambous, Irwin,
26 Bezodis, & Kerwin, 2012; Debaere, Delecluse, Aerenhouts, Hagman, & Jonkers, 2015;
27 Debaere et al., 2017; Mero, Kuitunen, Harland, Kyrolainen, & Komi, 2006). To perform these
28 calculations, a specific location of force application, termed the ‘centre of pressure’ (COP), is
29 required in addition to the ground reaction force (GRF) magnitude and direction, the position
30 and orientation of all segments within a rigid-body model, and the inertia parameters of these
31 segments (Winter, 2009). The COP is normally determined from the forces applied at each of
32 four triaxial transducers within a force platform (Winter, 2009).

33

34 Performance levels during the block clearance phase at the start of a race are strongly
35 associated with 100-m personal best times (Mero, 1988; Bezodis, Salo, & Trewartha, 2015;
36 Willwacher et al., 2016), and thus the block clearance phase is important for overall sprint
37 performance. To perform a lower extremity inverse dynamics analysis during this phase, the
38 COP on the starting block surface, rather than the ground level, is necessary. Although several
39 studies have calculated lower extremity joint torques during the block clearance phase using a
40 force platform embedded in the floor (Debaere et al., 2017; Mero et al., 2006; Otsuka,
41 Kurihara, & Isaka, 2015), these studies did not report how the COP on the starting block
42 surface was determined. Other studies of lower extremity joint torques during the block
43 clearance phase (Brazil et al., 2017, 2018) have used custom-made starting blocks which were
44 instrumented with four triaxial transducers in each block face (Willwacher, Küsel-Feldker,
45 Zohren, Herrmann, & Brüggemann, 2013), and similarly instrumented blocks are now
46 commercially available. In these studies, a ‘virtual landmark that projected the

47 metatarsophalangeal (MP) joint centre onto the surface of the block was used to define centre
 48 of pressure' (Brazil et al., 2017, p. 1631; 2018, p. 1657) on each block face. Although a
 49 projection from the MP joint provides an alternative way to estimate the COP when the COP
 50 cannot be directly obtained, this assumption would induce errors in the lower extremity joint
 51 torque calculations if the true COP is not located at this point. Moreover, using the MP joint
 52 location cannot provide the free moment at the COP. Using a simple coordinate
 53 transformation, the COP on a single starting block footplate which is independently secured
 54 on a force platform, as depicted in Figure 1, can be calculated theoretically by solving the
 55 following simultaneous equation:

56

$$57 \left(\begin{bmatrix} \vec{r}_x^{OB} \\ \vec{r}_y^{OB} \\ \vec{r}_z^{OB} \end{bmatrix} + \begin{bmatrix} a_{1,1} & a_{1,2} & a_{1,3} \\ a_{2,1} & a_{2,2} & a_{2,3} \\ a_{3,1} & a_{3,2} & a_{3,3} \end{bmatrix} \cdot \begin{bmatrix} \vec{r}_x^{BP} \\ \vec{r}_y^{BP} \\ \vec{r}_z^{BP} \end{bmatrix} \right) \times \begin{bmatrix} {}^O f_x \\ {}^O f_y \\ {}^O f_z \end{bmatrix} + \begin{bmatrix} a_{1,1} & a_{1,2} & a_{1,3} \\ a_{2,1} & a_{2,2} & a_{2,3} \\ a_{3,1} & a_{3,2} & a_{3,3} \end{bmatrix} \cdot \begin{bmatrix} 0 \\ 0 \\ {}^B n_z^{couple} \end{bmatrix} = \begin{bmatrix} {}^O n_x^{total} \\ {}^O n_y^{total} \\ {}^O n_z^{total} \end{bmatrix} \quad (1)$$

58

59 where \vec{r}_x^{OB} , \vec{r}_y^{OB} and \vec{r}_z^{OB} are coordinates of the origin of the starting block coordinate
 60 system (B) in the force platform (global) coordinate system (O), in which the origin is set at
 61 the centre of force platform at ground level; $a_{1,1}$ to $a_{3,3}$ are the components of a coordinate
 62 transformation matrix of the force platform coordinate system (O) to the starting block
 63 coordinate system (B); \vec{r}_x^{BP} , \vec{r}_y^{BP} and \vec{r}_z^{BP} are the coordinates of the COP (P) in the starting
 64 block coordinate system (B); ${}^O f_x$, ${}^O f_y$ and ${}^O f_z$ are applied forces onto the ground in the
 65 force platform coordinate system (O); ${}^B n_z^{couple}$ is the free moment applied on the x'y' plane
 66 of the starting block coordinate system (B); and ${}^O n_x^{total}$, ${}^O n_y^{total}$ and ${}^O n_z^{total}$ are applied
 67 moments around the origin of the force platform coordinate system (O). In the case where the
 68 COP (P) is on the x'y' plane of the starting block coordinate system (B), \vec{r}_z^{BP} is equal to zero.

69

70 The above-described equation makes it possible to define the COP using the coordinate
 71 system of the starting block, and GRFs and moments recorded on a force platform underneath

72 the block. Thus, this equation can be used in studies requiring the COP during the block
73 clearance phase, provided that the exact location of each starting block relative to an
74 independent force platform underneath is known (e.g. through direct measurement or the
75 attachment of markers). In this study, we firstly evaluated the accuracy of the aforementioned
76 calculation of the COP on the starting block. Secondly, we examined the influence of the COP
77 on the lower extremity joint kinetics to address the following hypothesis: there will be
78 differences in the lower extremity joint kinetics during the block clearance phase when
79 determining the COP using equation (1) compared with when determining it from a projection
80 from the MP joint. If the suggested calculation is valid and our hypothesis is accepted, these
81 methods will be important for use in future studies which calculate joint kinetics during the
82 block clearance phase in sprinting.

83

84 **Methods**

85 This study was conducted in two stages. Firstly, the accuracy of the new method to calculate
86 COP was determined by applying force onto multiple known locations on the starting block.
87 Secondly, to address our hypothesis, the influence of different COP calculations on the lower
88 extremity joint kinetics was investigated with data collected during the sprint start. This study
89 was approved by the Ethics Committee of the National Institute of Fitness and Sports in
90 Kanoya, Japan.

91

92 *Accuracy of centre of pressure location*

93 GRF during the test was recorded using a force platform which has four strain gauge force
94 transducers (0.32×1.2 m [width \times length]; TF-32120, Tec Gihan, Kyoto, Japan; 1000 Hz;
95 accuracy $< 1\%$; crosstalk $< 2\%$; natural frequency being >185 Hz for the vertical direction
96 and >220 Hz for the anteroposterior and mediolateral directions). A starting block rail (Super
97 III NF155B, Nishi, Tokyo, Japan), which is permitted for use in official races, was bolted at

98 four locations to the force platform covered by athletic track surface as depicted in Figure 2.
99 Thus, the block itself could be relocated easily, and in exactly the same ways as which it could
100 in a race.

101

102 One experimenter used a rod with a pointed tip to apply force at 18 specific locations on the
103 starting block in each of three block positions (forward, middle and back on the rail [M1 in
104 Figure 3 was 0.49, 0.28 and 0.08 m in the anteroposterior direction and consistently -0.09 m
105 in the mediolateral direction from the centre of the force platform]) and at two different block
106 angles (low and high inclinations [44.5 and 57.2° between the upper surface and the level
107 ground]) (in total, 6 conditions and 108 trials). The experimenter pressed the block surface
108 with maximal effort (resultant force being 372.2 ± 20.9 N) at an angle of approximately 55°
109 from the ground in the sagittal plane, which is representative of the mean angle of force
110 application against the starting blocks (Rabita et al., 2015).

111

112 Before applying force to the block surface, the locations of the force application were
113 determined using a motion capture system (Raptor-E, Motion Analysis Corporation, Santa
114 Rosa, CA, USA; 250 Hz, 10 cameras) for each condition. Small retro-reflective markers (11
115 mm in diameter) were affixed to the surface of the starting block at 18 specific locations (Figs.
116 2 and 3), after which they were removed and forces were applied to the locations under the
117 markers (the distance from the centre of the marker to the block surface was 6 mm and was
118 accounted for in subsequent calculations).

119

120 Using the marker coordinates on the starting block, recorded raw GRF, and moment data
121 around the centre of the force platform at ground level, COP values on the surface of the
122 starting block were calculated using equation (1). COP values were calculated by separating
123 the starting block surface in to three parts, using each of six markers on lower (M1 to M6),

124 middle (M7 to M12) and higher (M13 to M18) positions on the surface. In the case of the
 125 lower part, the origin of starting block coordinate system was set at M1 in Figure 3. The
 126 Y-axis (y') of the lower part of the starting block's coordinate system was defined by the
 127 vector running from M1 to M3 in Figure 3. The Z-axis (z') of the lower part of the starting
 128 block's coordinate system was defined as the vector product of the vector running from M1 to
 129 M4 and y' in Figure 3. The X-axis (x') of the lower part of the starting block's coordinate
 130 system was defined as the vector product of y' and z' . In the case of the lower part of the
 131 starting block's coordinate system, inputs for coordinate transformation in equation (1) were
 132 as follows:

133

$$134 \begin{bmatrix} \vec{r}_x^{OB} \\ \vec{r}_y^{OB} \\ \vec{r}_z^{OB} \end{bmatrix} = \begin{bmatrix} M1_x \\ M1_y \\ M1_z \end{bmatrix} \quad (2)$$

135 where M1 is the coordinate of the M1 marker in Figure 3.

136

$$137 \begin{bmatrix} a_{1,1} & a_{1,2} & a_{1,3} \\ a_{2,1} & a_{2,2} & a_{2,3} \\ a_{3,1} & a_{3,2} & a_{3,3} \end{bmatrix} = \begin{bmatrix} x'_x & y'_x & z'_x \\ x'_y & y'_y & z'_y \\ x'_z & y'_z & z'_z \end{bmatrix} \quad (3)$$

138

139 where x' , y' and z' indicate the coordinate system of the lower part of the starting block.
 140 Because all variables except for \vec{r}_x^{BP} , \vec{r}_y^{BP} and ${}^B n_z^{couple}$ are known (\vec{r}_z^{BP} is 6 mm as the
 141 height of the centre of the markers from the starting block surface), equation (1) can be solved,
 142 and \vec{r}_x^{BP} , \vec{r}_y^{BP} and ${}^B n_z^{couple}$ can be obtained. COP values and free moments in the middle
 143 and higher parts of the starting block were calculated using the same procedure with their
 144 origins at M7 and M13, respectively (Fig. 3).

145

146 The COP calculated using equation (1) with the force platform data for each location for 1 s
 147 during the middle of the force application duration was averaged for statistical analysis.

148 Means and standard deviations for values obtained by both the new method and reference
149 values, as well as the difference between the two, were reported for all variables. Moreover,
150 95% limits of agreement (LoA) between values from the new method and the reference values
151 were calculated.

152

153 *Comparison of the lower extremity joint kinetics*

154 Two male sprinters participated in this study (age, both 20 yrs; stature, 1.75 and 1.72 m; body
155 mass, 61.5 and 63.6 kg). The participants gave written informed consent before participating
156 in this study. After a self-directed warm-up, the participants, wearing their own spiked shoes,
157 performed three maximal effort 3 m sprints from starting blocks (their feet were only in
158 contact with starting blocks throughout the block clearance phase; no part of the foot touched
159 the ground). Lower extremity motion was recorded using a motion capture system (Raptor-E,
160 Motion Analysis Corporation, Santa Rosa, CA, USA; 250 Hz, 10 cameras). GRF and moment
161 underneath the right block during the block clearance phase were measured using the same
162 force platform mentioned above. The block used was the front block for one participant and
163 the rear block for the other. The locations and block angles were front low and middle high
164 for each respective participant.

165

166 Markers were affixed to the toes (superior aspect of the distal ends of the shoes), the posterior
167 aspect of the calcanei, the medial and lateral aspects of the first and fifth metatarsal heads,
168 respectively, malleoli, femoral condyles, greater trochanters, anterior superior iliac spines, and
169 posterior superior iliac spines. Segment endpoints were calculated from the three-dimensional
170 coordinates of the markers to create a 7-segment body model consisting of feet, shanks, thighs
171 and pelvis. Markers affixed to the toes and the posterior aspect of the calcanei were attached
172 to the spiked shoes and were considered as endpoints of the feet segments. The midpoints of
173 the markers affixed to the malleoli and femoral condyles were taken as the joint centres of the

174 ankles and knees, respectively. The midpoints of the markers affixed to the first and fifth
175 metatarsal heads were considered as the MP joint centre. The hip joint centre was defined as
176 the point located 18% of the distance between the right and left great trochanters medially
177 from the point located at one-third of the distance from the greater trochanter to the anterior
178 superior iliac spine (Nagahara, Matsubayashi, Matsuo, & Zushi, 2014).

179

180 The segment endpoint coordinates and GRF, as well as moments around the centre of the
181 force platform, were smoothed with a fifth-order spline filter (Woltring, 1986). The cut-off
182 frequency for all data was standardised as 20 Hz (Bezodis, Salo, & Trewartha, 2013;
183 Kristianslund, Krosshaug, & van den Bogert, 2012). Joint torques at the hip, knee and ankle
184 during the block clearance were calculated using a standard inverse-dynamics analysis for the
185 right leg (Winter, 2009). The moments applied around segmental centres of mass were
186 initially calculated by differentiating each segment's angular momentum in the global
187 reference frame. Subsequently, joint torques during the block clearance phase were computed
188 from the lower-extremity kinematics, kinetics and body segment inertia properties based on
189 an analysis of free-body-diagrams for each segment. The location of the centre of mass and
190 the inertia parameters of the respective segments were estimated from the body segment
191 parameters of Japanese athletes (Ae, 1996).

192

193 COP values for the inverse dynamics analysis were obtained using two methods: One was the
194 new method based on equation (1), and the other was determined from the location of the MP
195 joint centre. In the COP calculation using force platform data, five coordinate systems (the
196 origin being M1, M4, M7, M10 and M13 in Fig. 3) on the starting block surface were set.
197 When the COP moved below the origin of the used coordinate system, the coordinate system
198 for calculating the COP was changed to the lower one. For the COP estimation from the MP
199 joint coordinate, a location that projected the MP joint centre onto the surface of the block

200 was used based on the approach of Brazil et al. (2017; 2018). Although not stated in the
201 papers by Brazil et al. (2017, 2018), personal communications with the lead author of those
202 studies revealed that the MP joint centre was projected perpendicularly onto the
203 aforementioned block surface coordinate system to estimate the COP location. When the
204 estimated COP moved below the origin of the used coordinate system, the coordinate system
205 for estimating COP from the MP joint centre was changed to the lower one. The start of force
206 production on the starting block was determined using the first derivative of the GRF applied
207 perpendicularly to the block surface with a threshold of >500 N/s (Brazil et al., 2017). Toe-off
208 was defined when the GRF applied perpendicularly to the block surface next fell below 50 N
209 (Brazil et al., 2017). Average positive (extensor / plantar flexor) and negative (flexor /
210 dorsiflexor) torques at the hip, knee and ankle joint were calculated for each trial, and the
211 means and standard deviations across the three trials were determined. This provided
212 consistency with the average positive torques included in the performance-determinant
213 analysis of Brazil et al. (2018), and enabled quantification of some of the gross differences in
214 joint torques between the two methods in addition to a qualitative interpretation of the torque
215 time-histories at each joint. All the joint torque variables were expressed as mass specific
216 values. Cohen's d was used to determine the effect size (ES) of the difference between joint
217 torques calculated using the COP obtained by the new method and by the estimation from the
218 MP joint location (Cohen, 1988). Threshold values for the interpretation of the ES were <0.2
219 (trivial), $0.2 - <0.6$ (small), $0.6 - <1.2$ (moderate), and ≥ 1.2 (large) (Hopkins, Marshall,
220 Batterham, & Hanin, 2009).

221

222 **Results**

223 Table 1 shows the accuracy of the new method for calculating the COP, compared with the
224 reference values. The mean differences in the COP between the reference and new method in
225 the X, Y and Z axes were 0.002, -0.001 and 0.002 m, respectively. Moreover, the 95% LoA of

226 the COP was $< \pm 0.006$ m for all directions.

227

228 Figure 4 shows the differences in the hip, knee and ankle joint torques in the sagittal plane
229 from calculations using the COP values obtained by the new method and by the estimation
230 from the MP joint location. For both participants (right leg on the front and rear block,
231 respectively), hip and ankle joint torques calculated with the COP location estimated from the
232 MP joint location were overestimated and then underestimated during the respective first and
233 second halves of the force production durations during the block clearance phase. In contrast,
234 knee joint torque calculated with the COP location estimated from the MP joint location for
235 both participants were underestimated and then overestimated during the respective first and
236 second halves of the force production durations during the block clearance phase.

237

238 Table 2 shows mean positive and negative hip, knee and ankle joint torques in the sagittal
239 plane during the block clearance phase calculated using the COP values obtained by the new
240 method and by the estimation using MP joint location for two participants who used the right
241 leg as the rear and front leg on the block, respectively. Among the mean joint torque variables,
242 positive and negative knee joint torque of the front leg (difference = $39.9 \pm 17.5\%$ and -24.9
243 $\pm 33.1\%$, ES = 1.50 and 1.69) and positive ankle joint torque of the front leg (difference =
244 $-10.5 \pm 6.9\%$, ES = 2.04), as well as negative knee and positive ankle joint torques
245 (difference = $-25.3 \pm 7.1\%$ and $-7.2 \pm 1.6\%$, ES = 1.75 and 4.01) of the rear leg, showed
246 large differences between the calculations using the COP values obtained by the new method
247 and by the estimation using MP joint location.

248

249 Figure 5 shows the trajectories of the COP on the block surface obtained by the new method
250 and by the estimation from the MP joint location for all trials. For both participants (right leg
251 on the front and rear block, respectively), ranges of COP trajectories estimated from the MP

252 joint location were considerably smaller than the ranges of COP trajectories calculated from
253 the force platform data using the new method. Moreover, while the COP calculated using the
254 new method initially moved backward on the block surface, the COP estimated using the MP
255 joint location did not show this characteristic translation.

256

257 **Discussion and implications**

258 To our knowledge, this is the first study which has examined the accuracy of COP calculation
259 on an athletic starting block using data obtained by a force platform, and which has
260 established the influence of COP calculation methods on joint kinetics during the block
261 clearance phase. The calculated COP using the new method based on equation (1) was
262 accurate - it showed a mean bias of less than 2 mm and a random error (95% LoA) of less
263 than ± 6 mm when compared with reference COP locations determined using a motion capture
264 system. Our hypothesis was then accepted as there were some large differences in the lower
265 extremity joint torques during the block clearance phase when determining the COP using
266 equation (1) compared with when determining it from a projection from the MP joint.

267

268 The < 2 mm bias for the COP calculated by the new method is small in the context of the
269 distance moved by the COP on both of the blocks during the block clearance phase (Fig. 5),
270 demonstrating the high relative accuracy of the new method for calculating the COP on the
271 starting block. This bias also compares well with other values presented for novel COP
272 determination methods during overground sprinting, such as 3 mm when combining COP data
273 from two adjacent force platforms (Exell, Gittoes, Irwin, & Kerwin, 2012). Exell et al. (2012)
274 reported that their bias in COP calculation equated to a change in joint torques ranging from
275 0.6% for the hip to 1.4% for the ankle in the sagittal plane during maximal speed sprinting.
276 Based on these results, they concluded that the biases were sufficiently accurate, particularly
277 in the context of errors in other inverse dynamics inputs (e.g. noise in kinematic data) for

278 calculating joint torques (Exell et al., 2012). This provides further confidence that the new
279 method for calculating COP is sufficiently accurate for use in inverse dynamics analysis.
280 Using accurate COP values is very important for calculating net joint torque and power, as
281 well as the contribution of muscular contractions to the body acceleration. Thus, our new
282 method to obtain the COP on the starting block will enable more accurate calculation of joint
283 kinetics during the block clearance phase.

284

285 Time-histories of the leg joint torques during the block clearance phase calculated using the
286 COP estimated by MP joint location were visually different from those calculated using the
287 COP computed from force platform data using equation (1) (Fig. 4). In general, for both legs,
288 hip and ankle joint extensor and plantar flexor torques calculated using the COP estimated
289 from the MP joint location were initially over-estimated during the early part of the respective
290 pushing phase and then under-estimated during the second half of the respective pushing
291 phase (Fig. 4). The knee joint torque calculated using the COP estimated from the MP joint
292 location was under- and then over-estimated, during the respective first and second halves of
293 the force production durations during block clearance (Fig. 4). The mean joint torques during
294 the block clearance phase calculated using the COP estimated from the MP joint location
295 showed a large ($ES \geq 1.2$) under-estimation of ankle plantar flexion (7.2%) and knee flexion
296 torques (25.3%) of the rear leg (Table 2). Moreover, knee extension and flexion torques of the
297 front leg calculated using the COP estimated from the MP joint location were also largely
298 over- (39.9%) and under-estimated (24.9%), respectively (Table 2). These results demonstrate
299 that the calculation of joint torque using COP values estimated from the MP joint location
300 causes errors in the calculated leg joint torque, especially at the knee joint.

301

302 As all other input data for the inverse dynamics analysis remained the same, the
303 aforementioned over- and under-estimations of leg joint torques calculated using the COP

304 estimated from the MP joint location resulted from the smaller range of translation of the COP
305 compared with the true COP motion on the block surface (Fig. 5). During the first and second
306 halves of the force production duration during the block clearance phase, the COP estimated
307 from MP joint location was in front of and then behind the true COP calculated from the force
308 platform data. Moreover, the COP estimated from the MP joint location only showed a small
309 anterior motion compared with the more complex and initially posterior motion of the true
310 COP (Fig. 5). These errors in the COP estimated from the MP joint location therefore led to
311 the larger hip extension and ankle plantar flexion torques, as well as the smaller knee
312 extension torques, during the first half of the force production, and then the smaller hip
313 extension and ankle plantar flexion torques, as well as the larger knee extension torques,
314 during the second half of the force production of the block clearance phase. Whilst the general
315 patterns of the leg joint torque time-histories are consistent with those from previous studies
316 of the block clearance phase (Brazil et al., 2017; Mero et al., 2006), there are some important
317 differences. For example, Brazil et al. (2017) showed a flexor torque at the front knee during
318 the early part (~20-40%) of the block clearance phase, and a similar feature was evident in
319 this study when the COP was estimated from the MP joint location (Fig. 4e). Our new COP
320 calculation method has revealed that this knee flexor dominance, which is seemingly
321 counterintuitive given the demands of the movement, is in fact an artefact resulting from
322 errors in COP location, and that an extensor torque is dominant at the front knee joint
323 throughout the early part of the block clearance phase.

324

325 The current comparisons were undertaken as two case studies, and the equipment used (force
326 platforms under the blocks in our study versus instrumented starting blocks used by Brazil et
327 al., 2017; 2018), the participant ability levels (average 100 m personal best times of 11.20 s
328 versus 10.50 s) and the anteroposterior lengths of the starting blocks (0.25 m versus 0.15 m)
329 were also different between our study and the studies of Brazil et al. (2017; 2018). Whilst

330 these could lead to some differences in the observed COP locations between studies, the lower
331 extremity joint torque profiles estimated using the MP joint method in our study were
332 consistent with those from previous research (Brazil et al., 2017; Mero et al., 2006).
333 Furthermore, because we included our new COP calculation method as well as the exact one
334 used by Brazil et al. (2017; 2018) in our current study, confidence can be placed in the
335 generalisability of these findings. Where possible, based on the availability of separate block
336 footplates attached to independent force platforms, our new method should be applied when
337 the COP during the block clearance phase is required either as an outcome measure or as an
338 input to further calculations such as in an inverse dynamics analysis. In the case of a
339 commercially available instrumented starting block which can measure GRF and COP, as well
340 as free moment, in the block coordinate system, attaching markers to known locations on the
341 sides of the block will make it possible to obtain the location of COP and the GRF and free
342 moment vectors in the global coordinate system through coordinate transformation so that an
343 appropriate inverse dynamics analysis can be undertaken.

344

345 When multiple participants are recorded in one experimental session, the method used to
346 obtain locations and angles of the starting block in the current study will be challenging to
347 employ, because the block locations and angles are likely to be different between participants.
348 However, attaching markers to specific locations on the sides of the starting block will enable
349 these block settings to be determined. When the COP moves below the ground height based
350 on the calculation of the COP on the block, it is considered that the COP is located on the
351 level ground, and the calculation of COP can be done using the normal calculation on the
352 level ground. A further issue could arise if the toe contacts the ground and produces a free
353 moment on the ground when the COP is still on the starting block, as this will affect the
354 location of the COP calculated by the proposed method. However, the effect of the free
355 moment on the calculation of the COP is small, because the magnitude of the free moment is

356 considerably smaller than the magnitude of the GRF. Finally, whilst somewhat high
357 variabilities were evident in the difference in joint torques between the two methods (Fig. 4
358 and Table 2), these were primarily due to between-trial variability in performance (i.e. GRF
359 production). One specific example of this is evident in the rear ankle joint torques (Figure 4c)
360 - in the second trial, the participant produced a gradual increase in vertical force prior to
361 producing any horizontal force which thus influenced the identification of the onset of force
362 production (determined from the first derivative of the resultant force), explaining the
363 apparent delay in rear ankle torque production. Due to the method-validation focus of this
364 study, the participants were required to perform three maximal effort trials, but their levels of
365 performance or their satisfaction with each attempt were not assessed during data collection.
366 However, the between-trial variability evident in Table 2 serves to illustrate how the
367 assumption of the COP being a projection from the MP joint could lead to inconsistent errors
368 between trials as a result of typical variability in the forces produced by a sprinter.

369

370 **Conclusions**

371 This study validated a new method that can accurately determine the location of the centre of
372 pressure on a starting block during a sprint start using data from a force platform located
373 underneath the block. Moreover, comparison of the leg joint torques using this new method
374 against those determined using the centre of pressures estimated from the
375 metatarsophalangeal joint location demonstrates clear improvements and sometimes large
376 differences in the calculation of joint torques. These differences may have important
377 implications for the interpretation of joint kinetic strategies during the block clearance phase.

378

379 **Funding**

380 This research had no financial support to be conducted.

381

382 **Declaration of Conflicting Interests**

383 The authors declare that there is no conflict of interest.

384

385 **Reference**

- 386 Ae M. (1996). Body segment inertia parameters for Japanese children and athletes. *Japan*
387 *Journal of Sports Science*, *15*, 155–162.
- 388 Bezodis, N.E., Salo, A.I., & Trewartha, G. (2013). Excessive fluctuations in knee joint
389 moments during early stance in sprinting are caused by digital filtering procedures. *Gait*
390 *& Posture*, *38*, 653–657. doi: 10.1016/j.gaitpost.2013.02.015
- 391 Bezodis, N.E., Salo, A.I., & Trewartha, G. (2014). Lower limb joint kinetics during the first
392 stance phase in athletics sprinting: three elite athlete case studies. *Journal of Sports*
393 *Sciences*, *32*, 738–746. doi: 10.1080/02640414.2013.849000
- 394 Bezodis, N.E., Salo, A.I., & Trewartha, G. (2015). Relationships between lower-limb
395 kinematics and block phase performance in a cross section of sprinters. *European Journal*
396 *of Sport Science*, *15*, 118–124. doi: 10.1080/17461391.2014.928915
- 397 Brazil, A., Exell, T., Wilson, C., Willwacher, S., Bezodis, I., & Irwin, G. (2017). Lower limb
398 joint kinetics in the starting blocks and first stance in athletic sprinting. *Journal of Sports*
399 *Sciences*, *35*, 1629–1635. doi: 10.1080/02640414.2016.1227465
- 400 Brazil, A., Exell, T., Wilson, C., Willwacher, S., Bezodis, I., & Irwin, G. (2018). Joint kinetic
401 determinants of starting block performance in athletic sprinting. *Journal of Sports*
402 *Sciences*, *36*, 1656–1662. doi: 10.1080/02640414.2017.1409608
- 403 Charalambous, L., Irwin, G., Bezodis, I.N., & Kerwin, D.G. (2012). Lower limb joint kinetics
404 and ankle joint stiffness in the sprint start push-off. *Journal of Sports Sciences*, *30*, 1–9.
405 doi: 10.1080/02640414.2011.616948
- 406 Cohen, J. (1988). The t Test for Means. In J. Cohen (Ed.), *Statistical Power Analysis for the*
407 *Behavioral Sciences* (pp. 19–74). 2nd ed. Hillsdale, New Jersey: Lawrence Erlbaum
408 Associates.
- 409 Debaere, S., Delecluse, C., Aerenhouts, D., Hagman, F., & Jonkers, I. (2015). Control of
410 propulsion and body lift during the first two stances of sprint running: a simulation study.

411 *Journal of Sports Sciences*, 33, 2016–2024. doi: 10.1080/02640414.2015.1026375

412 Debaere, S., Vanwanseele, B., Delecluse, C., Aerenhouts, D., Hagman, F., & Jonkers, I.
413 (2017). Joint power generation differentiates young and adult sprinters during the
414 transition from block start into acceleration: a cross-sectional study. *Sports Biomechanics*,
415 16, 452–462. doi: 10.1080/14763141.2016.1234639

416 Exell, T.A., Gittoes, M.J., Irwin, G., & Kerwin, D.G. (2012). Considerations of force plate
417 transitions on centre of pressure calculation for maximal velocity sprint running. *Sports*
418 *Biomechanics*, 11, 532–541. doi: 10.1080/14763141.2012.684698

419 Hopkins, W.G., Marshall, S.W., Batterham, A.M., & Hanin, J. (2009). Progressive statistics
420 for studies in sports medicine and exercise science. *Medicine & Science in Sports &*
421 *Exercise*, 41, 3–13. doi: 10.1249/MSS.0b013e31818cb278

422 Kristianslund, E., Krosshaug, T., & van den Bogert, A.J. (2012). Effect of low pass filtering
423 on joint moments from inverse dynamics: implications for injury prevention. *Journal of*
424 *Biomechanics*, 45, 666–671. doi: 10.1016/j.jbiomech.2011.12.011

425 Mero, A. (1988). Force-time characteristics and running velocity of male sprinters during the
426 acceleration phase of sprinting. *Research Quarterly for Exercise and Sport*, 59, 94–98.
427 doi: 10.1080/02701367.1988.10605484

428 Mero, A., Kuitunen, S., Harland, M., Kyrolainen, H., & Komi, P.V. (2006). Effects of
429 muscle-tendon length on joint moment and power during sprint starts. *Journal of Sports*
430 *Sciences*, 24, 165–173. doi: 10.1080/02640410500131753

431 Nagahara, R., Matsubayashi, T., Matsuo, A., & Zushi, K. (2014). Kinematics of transition
432 during human accelerated sprinting. *Biology Open*, 3, 689–699. doi:
433 10.1242/bio.20148284

434 Otsuka, M., Kurihara, T., & Isaka, T. (2015). Effect of a wide stance on block start
435 performance in sprint running. *PLoS One*, 10, e0142230. doi:
436 10.1371/journal.pone.0142230

437 Rabita, G., Dorel, S., Slawinski, J., Saez-de-Villarreal, E., Couturier, A., Samozino, P., &
438 Morin, J.B. (2015). Sprint mechanics in world-class athletes: a new insight into the limits
439 of human locomotion. *Scandinavian Journal of Medicine and Science in Sports*, 25, 583–
440 594. doi: 10.1111/sms.12389

441 Willwacher, S., Küsel-Feldker, M., Zohren, S., Herrmann, V., & Brüggemann, G.-P. (2013). A
442 novel method for the evaluation and certification of false start apparatus in sprint running.
443 *Procedia Engineering*, 60, 124-129. doi: 10.1016/j.proeng.2013.07.073

444 Willwacher, S., Herrmann, V., Heinrich, K., Funken, J., Strutzenberger, G., Goldmann, J.P.,
445 ...Brüggemann, G.-P. (2016). Sprint start kinetics of amputee and non-amputee sprinters.
446 *PLoS One*, 11, e0166219. doi: 10.1371/journal.pone.0166219

447 Winter, D.A. (2009). *Biomechanics and Motor Control of Human Movement* (pp. 109–110,
448 117–121, 176–199). 4th ed. New York, NY: John Wiley & Sons, Inc.

449 Woltring, H.J. (1986). A Fortran package for generalized, cross-validatory spline smoothing
450 and differentiation. *Advances in Engineering Software*, 8, 104–113. doi:
451 10.1016/0141-1195(86)90098-7

452
453

454 Table 1 Comparison of COP coordinates determined using equation (1) against the reference
 455 values (pre-recorded marker coordinates). The values are means and standard deviations
 456 across the 108 trials in 6 conditions, except for 95% LoA.

457

Variables [unit]	Reference (marker)	FP method	Bias	95% LoA
Mediolateral coordinate [m]	-0.059 ± 0.024	-0.056 ± 0.023	0.002 ± 0.001	<0.001 to 0.005
Anteroposterior coordinate [m]	0.213 ± 0.170	0.212 ± 0.172	-0.001 ± 0.003	-0.006 to 0.003
Vertical coordinate [m]	0.084 ± 0.048	0.085 ± 0.048	0.002 ± 0.003	-0.003 to 0.006

458

459 LoA, limits of agreement

460

461

462

463 Table 2 Comparison of mean positive (extensor / plantar flexor) and negative (flexor /
 464 dorsiflexor) leg joint torques during the block clearance for each participant (one who used
 465 the right leg as the rear leg [Rear], and one who used the right leg as the front leg [Front] on
 466 the starting block). The values are means and standard deviations of three trials for each
 467 participant, except for ES.

468
 469

Variables [unit]		COP	MP	Difference	%Difference	ES	
Rear	Positive torque [Nm/kg]	Hip	1.44 ± 0.10	1.36 ± 0.10	-0.08 ± 0.02	-5.7 ± 1.1	0.78
		Knee	0.25 ± 0.06	0.28 ± 0.05	0.03 ± 0.03	-12.4 ± 13.4	0.48
		Ankle	0.68 ± 0.01	0.63 ± 0.01	-0.05 ± 0.01	-7.2 ± 1.6	4.01
	Negative torque [Nm/kg]	Hip	-0.12 ± 0.09	-0.13 ± 0.08	-0.01 ± 0.01	16.3 ± 20.4	0.11
		Knee	-0.30 ± 0.04	-0.22 ± 0.05	0.07 ± 0.01	-25.3 ± 7.1	1.75
		Ankle	-0.01 ± 0.01	-0.02 ± 0.02	-0.01 ± 0.01	140.1 ± 194.0	0.83
Front	Positive torque [Nm/kg]	Hip	1.83 ± 0.03	1.80 ± 0.09	-0.03 ± 0.06	1.9 ± 3.5	0.51
		Knee	0.84 ± 0.12	1.18 ± 0.31	0.35 ± 0.19	39.9 ± 17.5	1.50
		Ankle	0.95 ± 0.07	0.85 ± 0.02	-0.10 ± 0.07	-10.5 ± 6.9	2.04
	Negative torque [Nm/kg]	Hip	-1.29 ± 0.06	-1.33 ± 0.10	-0.04 ± 0.05	3.0 ± 3.6	0.48
		Knee	-0.32 ± 0.06	-0.23 ± 0.05	0.09 ± 0.11	-24.9 ± 33.1	1.69
		Ankle	0	0	0	0	

470
 471
 472
 473

ES, effect size calculated using Cohen's d.

474 **Figure captions**

475

476 Figure 1 Schematic of the coordinate transformation from the force platform coordinate
477 system (*O*) to the starting block coordinate system (*B*) for calculating the COP and free
478 moment on the starting block using the GRF and moment data collected by the force platform.

479

480 Figure 2 Depiction of the experimental set-up for the COP validation study including the force
481 platform, starting block and rail, and markers on the starting block.

482

483 Figure 3 Schematic of marker locations on the starting block for the COP validation study. M1
484 to M18 indicate marker names.

485

486 Figure 4 Hip, knee and ankle joint torques in the sagittal plane for all three trials of each
487 participant calculated using the COP locations obtained by the new method (solid lines) and
488 by the estimation using the MP joint projection (dotted lines). The upper row shows (a) hip,
489 (b) knee and (c) ankle joint torques of the right leg on the rear block for participant 1, while
490 the bottom row shows (d) hip, (e) knee and (f) ankle joint torques of the right leg on the front
491 block for participant 2. Light grey, dark grey and black lines indicate the first, second and
492 third trials, respectively.

493

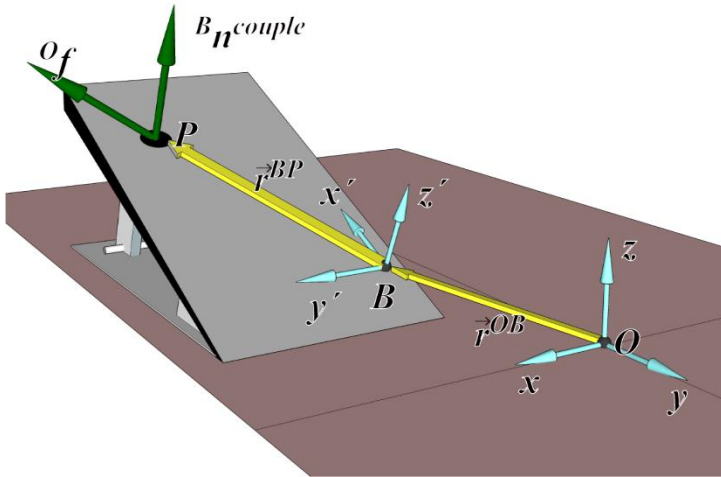
494 Figure 5 COP locations on the starting block surface for two participants calculated using the
495 force platform data with the new method (solid line) and estimated from the MP joint location
496 (dotted line). The left three panels show COP locations for the right leg on the rear block
497 (participant 1), while the right three panels show COP locations for the right leg on the front
498 block (participant 2). ‘Start’ and ‘end’ indicate the start of force production and the toe-off,
499 respectively. The origin in each panel is location M7 (see Fig. 3).

500

501

502 Figure 1

503



504

505

506 Figure 2

507



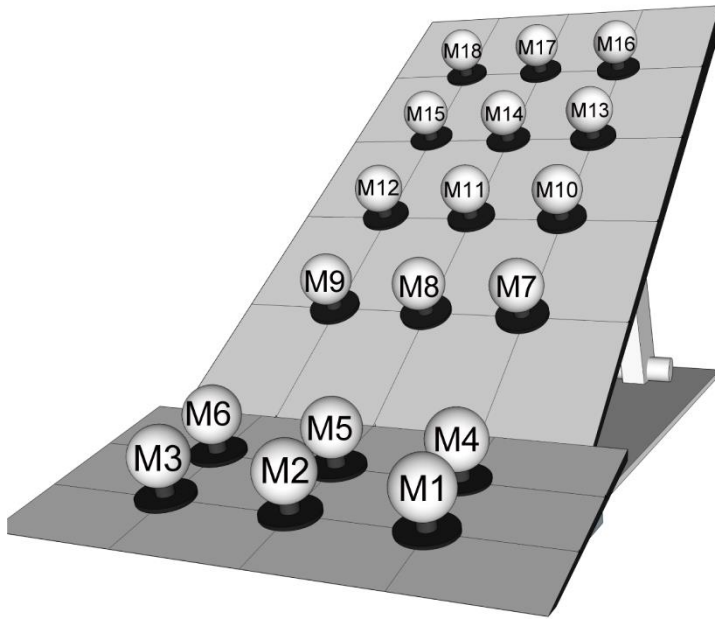
508

509

510

511 Figure 3

512

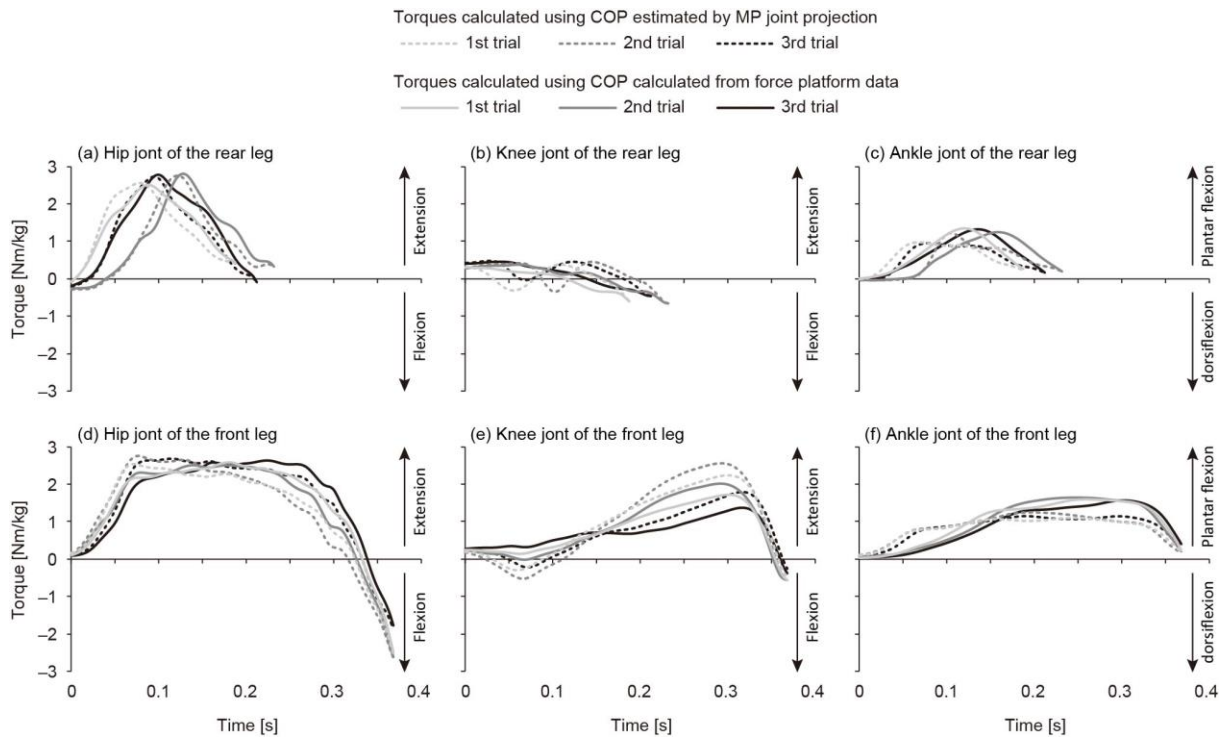


513

514

515 Figure 4

516

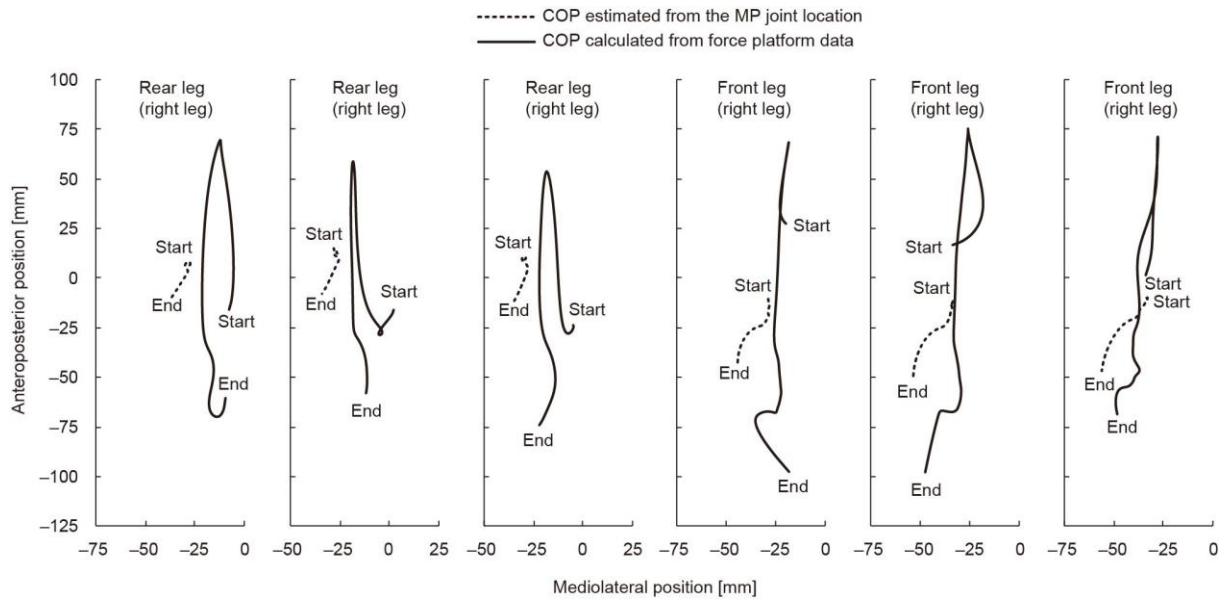


517

518

519 Figure 5

520



521